



## Effects of Cold Rolling and Annealing Time on Fatigue Resistance of AA5052 Aluminum Alloy

Kusmono\*, C. Bora, U. A. Salim

Department of Mechanical and Industrial Engineering, Faculty of Engineering, Universitas Gadjah Mada, Indonesia

### PAPER INFO

#### Paper history:

Received 16 May 2021  
Received in revised form 29 July 2021  
Accepted 02 August 2021

#### Keywords:

AA5052 Aluminum Alloy  
Cold Rolling  
Annealing  
Fatigue Resistance

### ABSTRACT

In the present study, the influences of cold rolling and annealing time on the fatigue crack propagation behavior of AA5052 aluminum alloy were investigated. The alloy sheet was cold-rolled under different rolling reductions, i.e., 0, 15, 30, and 45%. A 45% as-rolled specimen was then annealed at 370°C under different annealing times, i.e., for 2, 4, and 6 h. The microstructure evolutions after the cold rolling and annealing treatments were also examined using optical microscopy whereas the fatigue crack propagation behavior was characterized by using a fatigue test. Results showed that severely elongated grains were observed with increasing the rolling reduction. The elongated microstructures were changed into equiaxial structures due to recrystallization during annealing treatment. The fatigue life was decreased drastically by increasing the rolling reduction but increased significantly with increasing annealing time. The fatigue life of the alloy was reduced by 93% when cold-rolled up to 45%. On the other hand, the fatigue life of the 45% rolled samples was increased significantly by 412% when annealed at 370°C for 6 h.

Doi: 10.5829/ije.2021.34.09c.16

## 1. INTRODUCTION<sup>1</sup>

Due to its excellent properties including lightweight, processability, physical characteristics, corrosion resistance, and low cost, aluminum-magnesium alloys have been widely applied in the aerospace, automotive, shipbuilding, and construction industries [1,2]. One of the most widely used Al-Mg alloys is the AA5052 aluminum alloy. However, this alloy is non-heat treatable in that its strength is not high enough to be used for structural applications [3]. To improve its mechanical properties, there are two well-known methods, namely micro-alloying and strain hardening [4]. It is reported that the mechanical characteristics of aluminum alloys can be improved by the application of severe plastic deformations (SPD) such as accumulative roll-bonding, cryogenic rolling, and equal channel angular pressing [5,6]. Cold rolling has been proven to be one of the most widely used methods of strain hardening for Al-Mg aluminum alloys due to its simplicity, ease of processing, and low cost. Cold rolling can significantly enhance the

strength and hardness of Al-Mg aluminum alloy because of the improved dislocation density [7]. However, the ductility of the cold-rolled aluminum alloys is lower which limits its application due to poor forming ability. Tabatabaie and Zarasvand [8] studied the influences of cold bulge forming speed on thickness reduction and tensile properties of aluminum alloys. Their results showed that the tensile and yield strength of aluminum alloys were increased after cold bulge forming. Moreover, a more uniform thickness was achieved by reducing the forming speed. To enhance the ductility, an annealing treatment is often applied for cold-rolled Al-Mg aluminum alloys [9]. In our previous studies [10], it was reported that the strength and hardness of AA5052 aluminum alloy were significantly improved with rolling reduction but the ductility decreased. Furthermore, the annealing process decreased both strength and hardness but increased ductility. Several factors play a role in the success of annealings such as temperature, holding time, and heating rate of the process.

\*Corresponding Author Institutional Email: [kusmono@ugm.ac.id](mailto:kusmono@ugm.ac.id)  
(Kusmono)

Manufacturing components made of AA5052 which are used in several applications such as aerospace, automotive, and shipbuilding are often subjected to cyclic loading which can result in fatigue failure. In connection with this, several researchers have conducted many studies on the fatigue behavior of AA5052 aluminum alloy. Azadi et al. [11] investigated the effects of various parameters (maximum temperature, dwell time, thermo-mechanical loading factor) on the out-of-phase thermo-mechanical fatigue lifetime of the A356.0 casting aluminum alloy. They found that the maximum temperature and thermo-mechanical loading factor had a more significant effect on the lifetime compared to the dwell time. Li et al. [4] studied the effect of annealing treatment on the microstructure, tensile strength, and fatigue crack propagation behavior of Al-Mg-Sc alloy sheets. The sheets were hot-rolled at 470°C with the 77% rolling reduction and then cold-rolled with 65% reduction. The sheets were then annealed at 340 and 500°C for 1 h. They found that the microstructure, tensile strength, and fatigue crack growth rate were greatly dependent on the annealing temperature. Studies on the fatigue resistance of 5083-O aluminum alloy cold-rolled in parallel (PD) and in vertical to rolling direction (VD) were done by Ma et al. [12]. It was reported that the fatigue resistance of PD specimens was lower than that of the VD specimen due to the primary crack propagation throughout the chain-shaped coarse inclusions in PD specimens. Mughrabi and Hoppel [13] demonstrated that the fatigue properties of metal alloys are strongly affected by physical metallurgical properties such as grain size. Grain size affects remarkably both fatigue-crack propagation characteristics of alloys. Mughrabi and Hoppel [13] and Kim and Bidwell [14] reported that a microstructure with a relatively larger grain size has a higher fatigue-crack-propagation threshold ( $\Delta K_{th}$ ) and lower crack-growth rate. Shou et al. [15] investigated the effect of grain size on the fatigue crack propagation behavior of the 2524-T3 aluminum alloy. They found that the increased fatigue resistance of alloys with larger grain sizes is due to crack closure induced by both surface roughness and plasticity. Research works on the fatigue characteristics of aluminum alloys have been studied extensively, but published data on the influences of cold rolling and annealing treatment of AA5052 aluminum alloy have been limited.

In this study, the AA5052 alloy sheet was cold-rolled with different rolling reductions, namely 15, 30, and 45%. The sample with 45% reduction was then annealed at 370°C for different holding times, namely 2, 4, and 6 h. This work, the influences of cold rolling and annealing time on the fatigue crack propagation characteristic of AA5052 aluminum alloy were discussed. The fatigue fracture surfaces of these alloys were also characterized.

## 2. MATERIAL AND EXPERIMENTAL

The material used in this study was an AA5052 plate with its chemical composition is given in Table 1. In this investigation, the plate with 3 mm in thickness was firstly homogenized at 470°C for 6 h with a heating rate of 5°C/min and then cooled in air. The homogenized sheet was then cold-rolled at room temperature under different rolling reductions, namely 0, 15, 30, and 45%. The cold-rolled sheet with 45% reduction was then annealed at 370°C for different times, i.e., 2, 4 and 6 h with a heating rate of 5°C/min. The schematic illustration of the cold rolling and annealing processes was presented in Figure 1.

The microstructures of as-received, cold-rolled, and annealed specimens were observed using optical microscopy in a short transverse direction. The analysis of phases was carried out using an X-ray diffractometer (X'pert MPD) with Cu K $\alpha$  X-ray source and 2 $\theta$  range from 20 to 90° at a scanning rate of 0.03°/s. The fatigue crack growth test was conducted by using a servo-hydraulic universal testing machine with the center-crack tension (CCT) specimens taken from the sheet in the rolling direction as shown in Figure 2. Electric discharge machining was used to prepare the notches and the surface of the sample under test was polished. All tests were carried out at a stress ratio of  $R = 0.1$ , and with a sinusoidal loading frequency of 11 Hz at room temperature. A 20% of yield stress was selected as stress level and the fatigue crack growth rate ( $da/dN$ ) of the Paris power law was determined following the Secant method below:

$$\left(\frac{da}{dN}\right)_{\bar{a}} = \frac{a_{i+1} - a_i}{N_{i+1} - N_i} \quad (1)$$

$$\bar{a} = \left(\frac{a_{i+1} + a_i}{2}\right) \quad (2)$$

where,  $\bar{a}$  is average crack length, subscripts  $i$  and  $(i + 1)$  represent  $i_{th}$  and  $(i + 1)_{th}$  cycle. The stress intensity factor range,  $\Delta K$  for center crack tension (CCT) geometry was determined as follows:

$$\Delta K = \frac{\Delta P}{B} \left[ \sqrt{\frac{\pi \alpha}{2W} \sec \frac{\pi \alpha}{2}} \right] \quad (3)$$

$$\Delta P = P_{max} - P_{min} \quad (4)$$

where  $P$  is the load,  $B$  and  $W$  are the thickness and width

**TABLE 1.** Chemical compositions of AA5052 aluminum alloy

| Chemical composition (wt.%) |      |      |      |      |      |
|-----------------------------|------|------|------|------|------|
| Mg                          | Fe   | Cr   | Si   | Mn   | Al   |
| 2.37                        | 0.31 | 0.22 | 0.11 | 0.08 | Bal. |

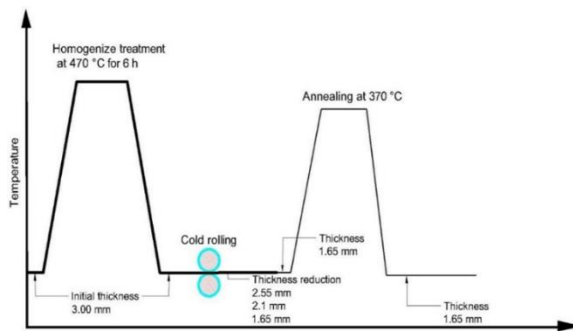


**Figure 1.** Schematic illustration of both cold rolling and annealing processes

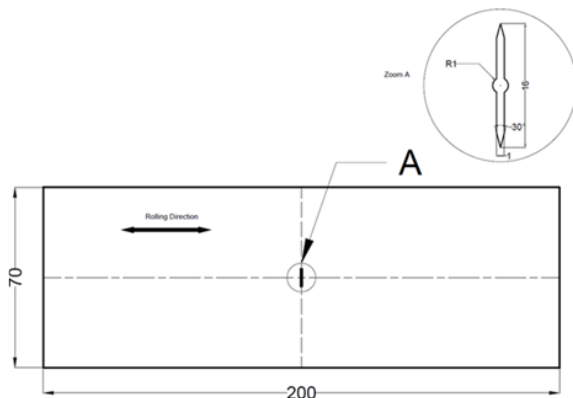


**Figure 2.** Centre-crack tension (CCT) specimen

of the sample, respectively;  $\alpha = 2a/W$ ; and  $a$  is the length of half of the crack. The fatigue fracture surface of the specimens was examined using scanning electron microscopy (Carl Zeiss Evo Ma 10 SEM).

### 3. RESULTS AND DISCUSSION

**3.1. Microstructure Observations** Figure 3a shows three principal directions in the alloy during cold rolling. Figures 3b, 3c, 3d, 3e, and 3f display the optical micrographs in the short transverse direction of as-received, as-rolled with 15, 30, 45% reduction, and as-rolled with 45% reduction followed by annealing for 6 h, respectively. The structure of the  $\alpha(\text{Al})$  matrix and many second phases dispersed within the grain are observed in all samples. Some equiaxed grains and elongated ones can be observed in Figure 3b. However, a larger elongated grain as a result of cold rolling is exhibited clearly in Figures 3c, 3d, and 3e. This indicates that the cold rolling led to a smaller grain size of alloy. An increase in the number of nucleation sites when higher rolling reductions are applied may be responsible for the smaller grain size [16]. Some equiaxed grains can be observed in the 45% as-rolled sample followed by annealing for 6 h in Figure 3f. This suggests that the

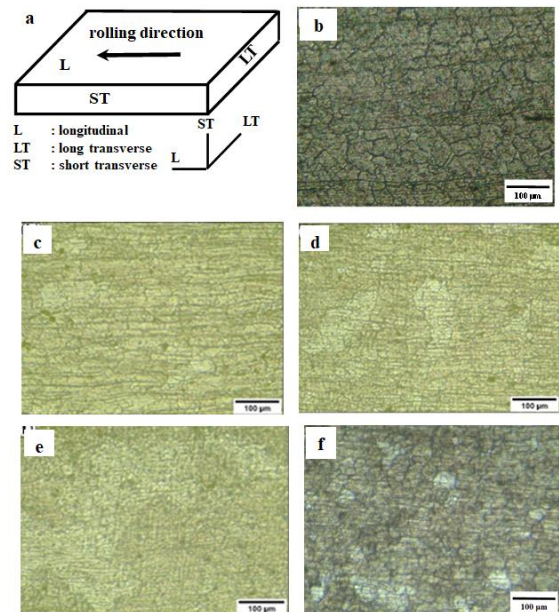


**Figure 3.** (a) Three principal directions in the alloy sheet with corresponding microstructure in short transverse: (b) as-received sample, (c) 15% as-rolled sample, (d) 30% as-rolled sample, (e) 45% as-rolled sample, (f) 45% as-rolled sample followed by annealing for 6 h

annealing for 6 h has changed from the elongated grains to the equiaxed ones. This may be related to the recrystallization phenomenon that occurred during annealing treatment [9].

**3.2. X-Ray Diffraction Analysis** The XRD patterns of as-received and as-rolled samples with different thickness reductions are demonstrated in Figure 4. As shown in Figure 4, it can be observed that both as-received and as-rolled samples consist of similar phases, namely  $\alpha(\text{Al})$  matrix, and  $\text{Al}_3\text{Fe}$ . No other phases were observed. This suggests that the cold rolling does not change the phases in the AA5052 aluminum alloy. However, the intensity of diffraction peaks is increased with rolling reduction, especially for 45% reduction. This indicates that the amount of secondary phase ( $\text{Al}_3\text{Fe}$ ) increases with increasing rolling reduction. An increase in cold rolling causes greater energy stored in the cold-rolled sample as indicated by an increase in the intensity of  $\text{Al}_3\text{Fe}$  as shown in the XRD results. In addition, cold rolling produces an increase in dislocation density. Similar observations were also demonstrated by previous researchers [9] where the cold rolling did not affect the microstructure but only increased the amount of the second phase as indicated by the enhanced intensity of peaks after cold rolling. Figure 5 displays the XRD patterns of as-rolled with 45% reduction and annealed samples for different holding times. It can be seen from

Figure 5 that all samples are composed of  $\alpha$  (Al matrix and  $Al_3Fe$  as shown in Figure 4. This implies that the annealing treatment at  $370^\circ C$  for 2, 4, and 6 h does not affect the phase changes of as-rolled AA 5052 aluminum alloy. The annealing time does not influence the presence of  $Al_3Fe$  because the annealing treatment reduces the dislocation density due to the recrystallization process during annealing treatment.

### 3. 3. Fatigue Crack Propagation Behavior

Results of fatigue tests of the as-received and as-rolled alloy under different rolling reductions are displayed in Figure 6. It was found that the fatigue life of as-received alloy was around 1,050,000 cycles. A remarkable reduction in fatigue life is exhibited by a 15% cold-rolled sample where the number of cycles decreased to around 560,000 cycles. More reduction in fatigue life is also found for as-rolled samples with the rolling reductions of 30 and 45%. The number of cycles of as-rolled specimens

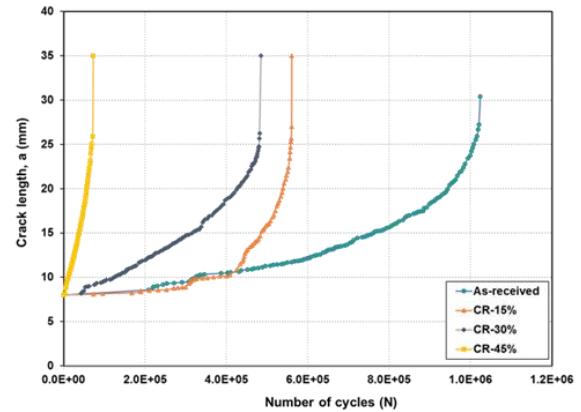


**Figure 6.** Fatigue life of as-received and as-rolled samples with different rolling reductions

with 30 and 45% reduction is 485,000 and 73,000 cycles, respectively. It can be concluded that the fatigue life of alloy is drastically reduced with rolling reduction. This is probably attributed to the smaller grain size and high tensile residual stress caused by cold rolling [17, 18]. These increases the local stress ratio and the effective stress intensity factor range and finally result in reduced fatigue life [18].

Figure 7 displays the fatigue crack growth rate as a function of the stress intensity factor range ( $\Delta K$ ) of as-received and as-rolled alloy with different rolling reductions. It is observed that the fatigue crack propagation curves reveal three different regions, i.e., I, II, and III. For both samples, region II shows a stable rate of fatigue crack growth following the Paris law as given by:

$$\frac{da}{dN} = C (\Delta K)^n \tag{5}$$

where  $da/dN$  is the growth rate of fatigue cracks, and  $\Delta K$  is the difference between the maximum and minimum stress intensity factors, ( $K_{max} - K_{min}$ ) during the load cycle. By taking the trend line in region II, the values of C and n known as the Paris constant can be determined and the results are presented in Figure 8 and summarized in Table 2. C is the value of  $da/dN$  at  $\Delta K = 1 \text{ MPa}\cdot\text{m}^{0.5}$  and n represents the slope of the lines. The n value of aluminum alloy increased with rolling reduction. This indicates that the cold rolling increased the fatigue crack growth rate. The reduced fatigue performance is ascribed to the smaller grain size and tensile residual stress induced by cold rolling. These findings were consistent with previous results reported that the rate of fatigue crack growth of fine-grained commercially pure titanium induced by the cold rolling was higher compared to that of the coarse-grained samples due to the difference in the magnitude of crack closure of the samples [19-21]. The rate of fatigue crack growth of aluminum alloys is greatly influenced by grain size [15,22]. It has been reported by previous researchers that the higher rate of fatigue crack

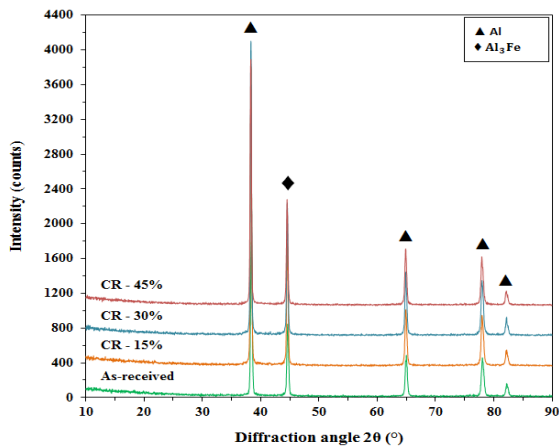


**Figure 4.** XRD patterns of as-received and as-rolled samples with different thickness reductions

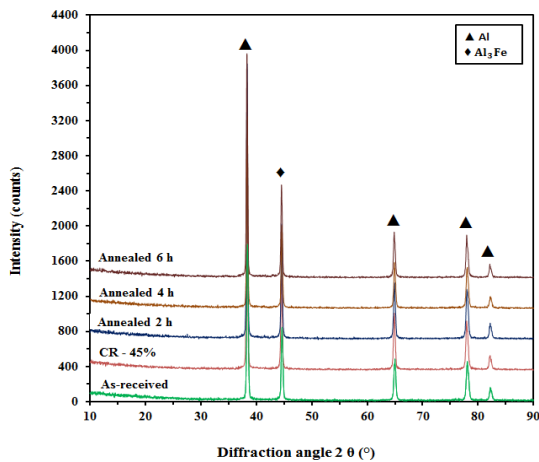


**Figure 5.** XRD patterns of as-rolled samples with 45% reduction subjected to annealing at different times

propagation was indicated by a smaller grain size compared to alloys with a larger grain size [23]. This is related to the combined effects of grain boundaries, crack deflection, and crack closure due to crack surface roughness and plasticity [15].

Figure 9 demonstrates the fatigue life of 45% as-rolled alloy with different annealing holding times. It is found that the fatigue life for samples annealed for 2, 4,

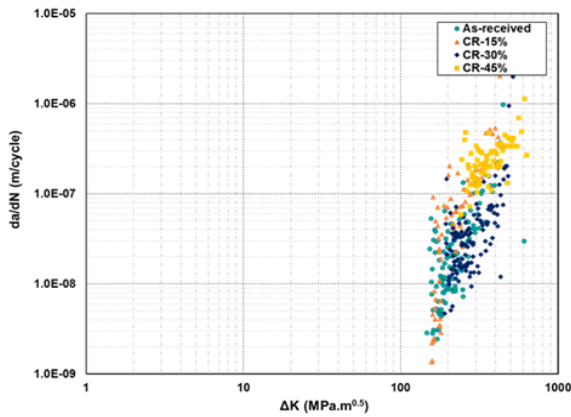


Figure 7. Fatigue crack propagation rate of as-received and as-rolled samples with different rolling reductions

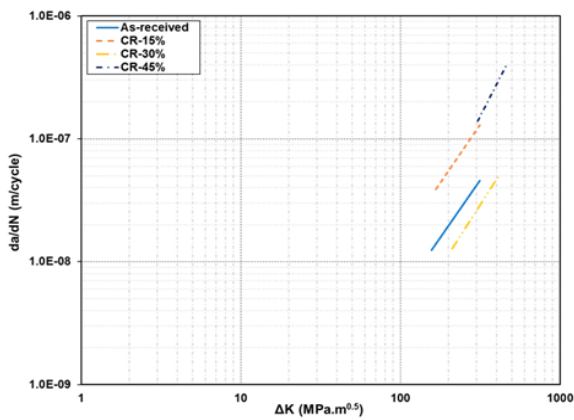


Figure 8. Trend line taken from region II of Figure 7

TABLE 2. Paris Constants of as-received, as-rolled samples and followed by annealing under different times

| Materials                 | C          | n      |
|---------------------------|------------|--------|
| As-received               | 9.6351E-13 | 1.8726 |
| CR-15%                    | 2.3555E-12 | 1.8979 |
| CR-30%                    | 2.4204E-13 | 2.0317 |
| CR-45%                    | 6.9064E-14 | 2.5379 |
| CR-45% + annealed for 2 h | 5.7237E-14 | 2.3969 |
| CR-45% + annealed for 4 h | 4.3521E-13 | 2.2841 |
| CR-45% + annealed for 6 h | 3.5767E-13 | 2.0028 |

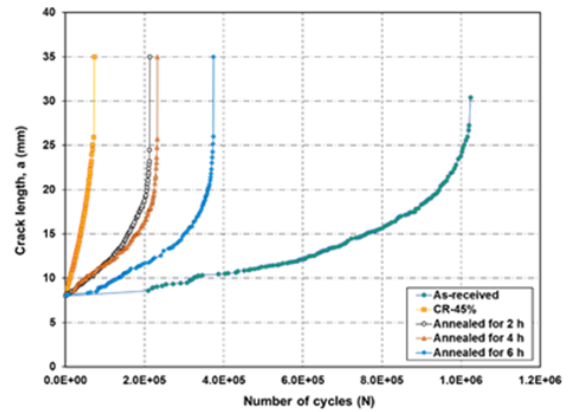


Figure 9. Fatigue life of as-received and as-rolled samples followed by annealing with different annealing times

and 6 h are 213,000, 232,000, and 374,000 cycles, respectively. Compared to the un-annealed sample, there is a significant increase in fatigue life by 192, 218, and 412% for samples annealed for 2, 4, and 6 h, respectively. This indicates that the annealing treatment significantly enhances the fatigue life of an as-rolled alloy. This may be due to the more ductile nature of the annealed alloy compared to the rolled sample allowing a greater number of crack extensions before failure [24]. In addition, these are also attributed to both the reduced dislocation density and tensile residual stress because of recrystallization during annealing [25].

Figure 10 demonstrates the fatigue crack growth rate as a function of stress intensity factor range ( $\Delta K$ ) of as-received and 45% as-rolled alloy for different annealing times. It can be seen that all samples also reveal the fatigue crack growth rate curves with three distinct regions, i.e., the region I, II, and III. All samples also exhibit the stable fatigue crack growth rate in region II and follow Paris law. The curve of  $da/dN$  versus  $\Delta K$  taken from region II is presented in Figure 11 and Paris constants are determined that summarized in Table 2.

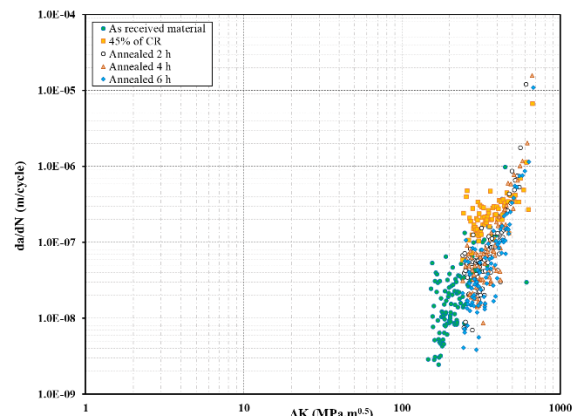
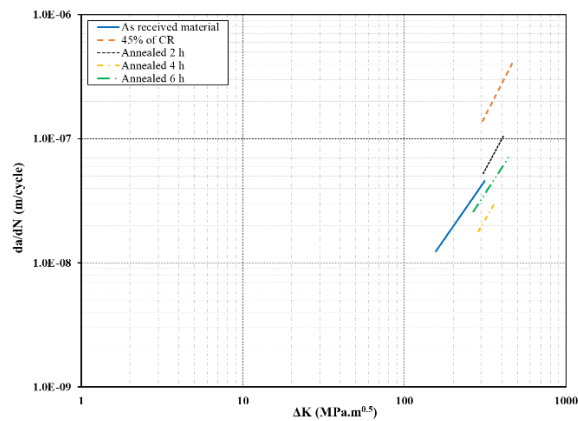


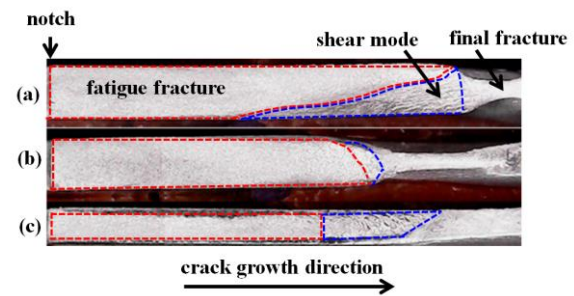
Figure 10. Fatigue crack propagation rate of as-received and 45% as-rolled samples with different annealing times



**Figure 11.** Trend line taken from region II of Figure 10

From Table 2, it can also be found that the  $n$  value is decreased with annealing time. This implies that the annealing treatment reduces the fatigue crack growth rate. This is associated with grain coarsening as a result of recrystallization during annealing. Furthermore, the grain coarsening can increase the intensity factor of the crack closure and decrease the driving force of change in the crack path. It is ascribed to the microstructure and possible contact between facets of rough cracks resulting in a low crack growth rate as indicated by lower  $n$  values after annealing treatment [26,27]. This may also be associated with the higher release rate of tensile residual stress with increasing annealing time producing a lower fatigue crack growth rate. In addition, The enhanced fatigue crack growth resistances for annealed alloys may be attributed to their high  $C$  values (but lower values of  $n$ ) suggesting that the fatigue crack growth retardation occurs at high  $\Delta K$  [28].

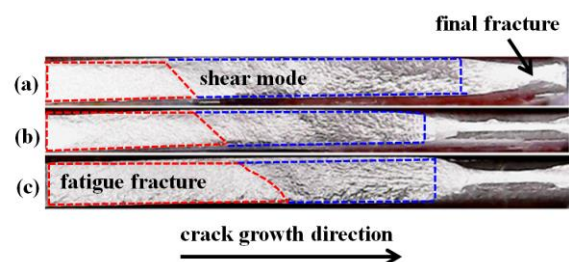
**3. 4. Fatigue Fracture Surface Analysis** Figure 12 shows the fatigue fractured surfaces of AA5052 aluminum alloy for as-received and as-rolled samples with 15 and 45% of rolling reduction. The crack propagates from the left to the right as shown in Figure 12 with the initial crack from the notch. From Figure 12, it can be seen that the fracture surface consisted of three different regions, namely an area with a flat surface that is characteristic of a fatigue fracture, an area with a rougher surface called a shear fracture or shear mode, and an area with a reduction in the area which is a feature of the final fracture. The fatigue surface area reflects the fatigue life of the fatigue-tested alloy [29]. Therefore, the larger the fatigue surface area confirms the higher the fatigue life. From Figure 12, it can be observed that the largest area of the fatigue fracture is observed for the as-received alloy followed by the cold-rolled alloy with 15% rolling reduction, and alloy with 45% rolling reduction. This confirms that the fatigue life of the alloy is reduced with an increase of rolling reduction as presented in Figure 6.



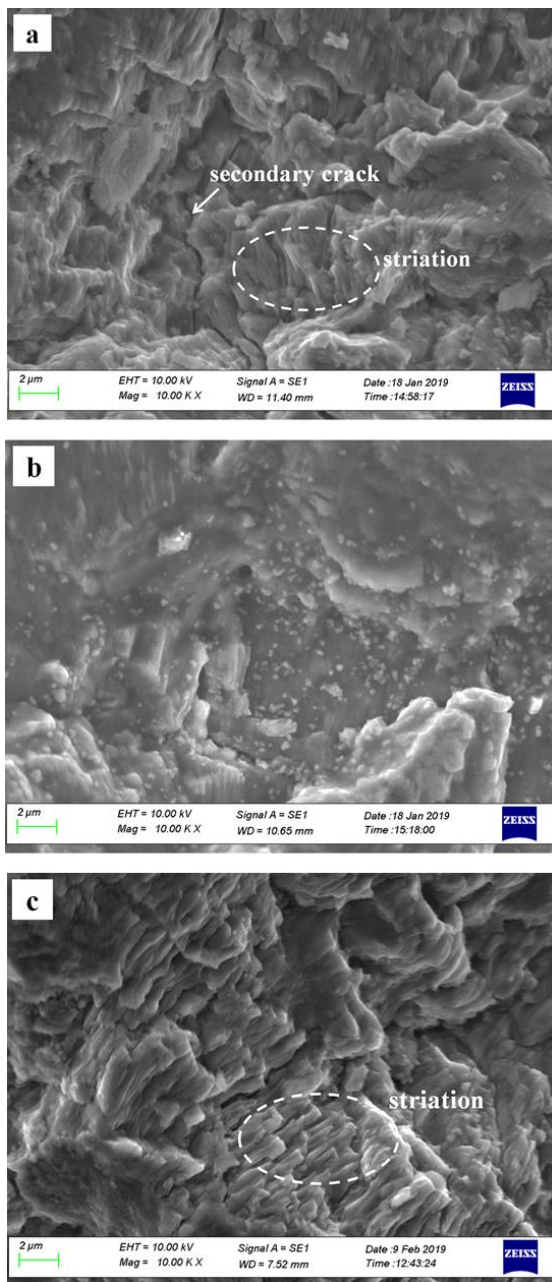
**Figure 12.** Fractured surfaces of AA 5052 aluminum alloy: (a) As-received, (b) CR-15%, (c). CR-45%

Figure 13 presents the fatigue fractured surfaces of AA 5052 aluminum alloys subjected to cold rolling with 45% and followed by annealing at different times of 2, 4, and 6 h. A similar to Figure 12, three different regions, namely the fatigue, shear, and final fractures can be observed. The larger area of the fatigue fracture is observed for the alloy annealed 6 h followed by 4 and 2 h. This suggests that the fatigue life of the alloy is increased with increasing annealing time. These results are consistent with the fatigue life as shown in Figure 9 before. From Figures 12 and 13, it can also be observed that the area of fatigue surface of the as-received alloy is still higher compared to that of all annealed alloys. This reflects that the fatigue life of as-received alloy is higher than that of cold-rolled alloy followed by annealing treatment at different times. In other words, the annealing treatment has not been able to restore the fatigue life of as-received alloy.

Figure 14 displays scanning electron micrographs of the fatigue fracture surfaces taken from stable crack propagation region of as-received, 45% as-rolled, and 45% as-rolled alloy annealed for 6 h. It can be seen that the presence of fatigue striation can be observed in the fatigue crack fractures of as-received and 45% as-rolled samples annealed for 6 h (Figures 14a and 14c). The smaller striation width can be seen in the fracture surface of the as-received sample compared to the 45% as-rolled alloy followed by annealing for 6 h. This supports the lower fatigue crack growth rate exhibited by the



**Figure 13.** Fractured surfaces of AA 5052 aluminum alloy subjected to 45% of cold rolling and annealed at different times: (a) 2 h, (b) 4 h, (c) 6 h



**Figure 14.** SEM images of fatigue fracture surfaces of (a) as-received alloy, (b) 45% as-rolled alloy, (c) 45% as-rolled alloy and annealed for 6 h

as-received sample compared to the 45% as-rolled sample annealed for 6 h, as shown in Figure 8 and Table 2. According to Matos et al. [30], striation width is the fatigue crack growth distance under each cyclic load reflecting the fatigue crack growth rate properly. In general, the smaller striation width corresponds to the lower fatigue crack growth rate [31,32]. Another feature seen in Figures 14a and 14c is the presence of the secondary crack obtained in the fracture surface of as-received and 45% as-rolled followed by annealing for 6

h. It is interesting to note from Figure 14b that poorly defined striation is revealed in the fatigue surface of 45% as-rolled AA5052 aluminum alloy. This indicates the transgranular cleavage fracture as typical of brittle fracture. This confirms the high fatigue crack propagation rate of 45% as-rolled AA 5052 aluminum alloy as shown in Figure 8 and Table 2.

#### 4. CONCLUSIONS

In this study, the effects of cold rolling and annealing time on the microstructure and fatigue behavior of the AA5052 aluminum alloy was investigated and the conclusions were as follows:

- The severely elongated grains are observed with increasing rolling reduction. The elongated microstructures are changed to equiaxial structures due to recrystallization during annealing treatment especially for an annealing holding time of 6 h.
- Both cold rolling and annealing processes do not change the phases in the AA5052 aluminum alloy.
- Both cold rolling and annealing time strongly influence the fatigue resistance of AA5052 aluminum alloy. The fatigue resistance decreases drastically as the rolling reduction increases. On the other hand, the fatigue resistance of cold-rolled AA5052 aluminum alloy increases significantly with increasing annealing time.

#### 5. ACKNOWLEDGEMENTS

The financial support from Universitas Gadjah Mada, Yogyakarta, Indonesia through the research grant of Rekognisi Tugas Akhir (RTA) Program 2019 (contract no. 2129/UN1/DITLIT/DIT-LIT/LT/2019) is greatly appreciated.

#### 6. REFERENCES

1. Xia, S.L., Ma, M., Zhang, J.X., Wang, W.X., Liu W.C. "Effect of heating rate on the microstructure, texture and tensile properties of continuous cast AA5083 aluminum alloy." *Materials Science and Engineering A*, Vol. 609, (2014), 168-176, <https://doi.org/10.1016/j.msea.2014.05.002>
2. Panagopoulos, C.N., Georgiou, E.P. "Cold rolling and lubricated wear of 5083 aluminium alloy." *Materials and Design*, Vol. 31, (2010), 1050-1055, <https://doi.org/10.1016/j.matdes.2009.09.056>.
3. Lin, S., Nie, Z., Huang, H., Li, B. "Annealing behavior of a modified 5083 aluminum alloy." *Materials and Design*, Vol. 31, (2010), 1607-1612, <https://doi.org/10.1016/j.matdes.2009.09.004>.
4. Li, M., Pan, Q., Shi, Y., Wang, Y. "Microstructure dependent fatigue crack growth in Al-Mg-Sc alloy." *Materials Science & Engineering A*, Vol. 611, (2014), 142-151, <https://doi.org/10.1016/j.msea.2014.05.087>.

5. Liu, J.T., Morris J. "Recrystallization microstructures and textures in AA 5052 continuous cast and direct chill cast aluminum alloy." *Materials Science and Engineering A*, Vol. 385, (2004), 342-351, <https://doi.org/10.1016/j.msea.2004.06.070>.
6. Daryadel, M. "Study on equal channel angular pressing process of AA7075 with copper casing by finite element-response Surface Couple Method." *International Journal of Engineering: Transactions C: Aspects*, Vol. 33, No. 12, (2020) 2538-2548, DOI:10.5829/ije.2020.33.12c.15.
7. Morrisa, D.G., Muñoz-Morrisa, M.A. "Microstructure of severely deformed Al-3Mg and its evolution during annealing." *Acta Materialia*, Vol. 50, No. 16, (2002), 4047-4060, [https://doi.org/10.1016/S1359-6454\(02\)00203-3](https://doi.org/10.1016/S1359-6454(02)00203-3).
8. Tabatabaiea, S.M.R., Zarasvand, K.A. "Investigating the effects of cold bulge forming speed on thickness variation and mechanical properties of aluminum alloys: Experimental and Numerical." *International Journal of Engineering, Transaction C: Aspects*, Vol. 31, No. 9, (2018), 1602-1608, DOI: 10.5829/ije.2018.31.09c.17.
9. Wang, B., Chen, X., Pan, F., Mao, J., Fang, Y. "Effects of cold rolling and heat treatment on microstructure and mechanical properties of AA 5052 aluminum alloy." *Transaction Nonferrous Metal Society of China* Vol. 25, (2015), 2481-2489, [https://doi.org/10.1016/S1003-6326\(15\)63866-3](https://doi.org/10.1016/S1003-6326(15)63866-3).
10. Kusmono, Bora, C., Salim, U.A. "Effects of cold rolling (CR) and annealing time on microstructure and mechanical properties of AA 5052 aluminum alloy." *Metallurgy*, Vol. 59, No. 4, (2020), 485-488.
11. Azadi, M., Farrahi, G.H., Winter, G., Eichlseder, W. "The effect of various parameters on out-of-phase thermo-mechanical fatigue lifetime of A356.0 cast aluminum alloy." *International Journal of Engineering: Transactions C: Aspects*, Vol. 26, No. 12, (2013), 1461-1470, DOI: 10.5829/idosi.ije.2013.26.12c.06.
12. Ma, M., Zhang, J., Yi, D., Wang, B. "Investigation of high-cycle fatigue and fatigue crack propagation characteristic in 5083-O aluminum alloy." *International Journal of Fatigue*, Vol. 126, (2019), 357-368, <https://doi.org/10.1016/j.ijfatigue.2019.05.020>.
13. Mughrabi H, Hoppel HW. Cyclic deformation and fatigue properties of ultrafine grain size materials: current status and some criteria for improvement of the fatigue resistance. *Material Research Society Symposium Proceedings*, (2001), 634. B2.1.1–B2.1.12.
14. Kim Y-W, Bidwell LR. Effects of microstructure and aging treatment on the fatigue crack growth behaviour of high strength P/M aluminum alloy X7091. In: High-strength powder metallurgy aluminum alloys: proceedings of a symposium sponsored by the Powder Metallurgy Committee of the Metallurgical Society of AIME, held at the 111th AIME Annual Meeting, Dallas, Texas, February 17–18, 1982/edited by Michael J. Koczak, Gregory J. Hildeman; 107-124.
15. Shou, W.B., Yi, D.Q., Liu, H.Q., Tang, C., Shen, F.H., Wang, B. "Effect of grain size on the fatigue crack growth behavior of 2524-T3 aluminum alloy." *Archive of Civil and Mechanical Engineering*, Vol. 16, (2016), 304-312, <https://doi.org/10.1016/j.acme.2016.01.004>.
16. Nah, J.J., Kang, H.G., Huh, M.Y., Engler, O." Effect of strain states during cold rolling on the recrystallized grain size in an aluminum alloy." *Scripta Materialia* Vol. 58, (2008), 500-503, <https://doi.org/10.1016/j.scriptamat.2007.10.049>.
17. Liu, S.Z., Minakawa, K., Scholtes, B., Mcevely, A.J. "The effect of cold rolling on the fatigue properties of Ti-6Al-4V." *Metallurgical Transactions A*, Vol. 16, (1985), 144-145, <https://doi.org/10.1007/BF02656725>.
18. Korsgren, P., Sperle, J.O., Trogen, H. "Influence of shearing and punching on the fatigue strength of hot rolled steel sheet." *Scandinavian Journal of Metallurgy*, Vol. 18, (1989), 203-210.
19. Kikuchi, S., Mori, T., Kubozono, H., Nakai, Y., Kawabata, M.O., Ameyama, K. "Evaluation of near-threshold fatigue crack propagation in harmonic-structured CP titanium with a bimodal grain size distribution." *Engineering Fracture Mechanics*, Vol. 181, (2017), 77-86, <https://doi.org/10.1016/j.engfractmech.2017.06.026>.
20. Kikuchi, S., Ueno, A., Akebono, H. "Combined effects of low temperature nitriding and cold rolling on fatigue properties of commercially pure titanium." *International Journal of Fatigue*, Vol. 139, (2020), 105772, <https://doi.org/10.1016/j.ijfatigue.2020.105772>.
21. Nakai, Y., Kikuchi, S., Osaki, K., Kawabata, M.O., Ameyama, K. "Effects of rolling reduction and direction on fatigue crack propagation in commercially pure titanium with harmonic structure." *International Journal of Fatigue*, Vol. 143, (2021), 106018, <https://doi.org/10.1016/j.ijfatigue.2020.106018>.
22. Yin, D., Liu, H., Chen, Y., Yi, D., Wang, B., Shen, F., Fu, S., Tang, C., Pan, S. "Effect of grain size on fatigue-crack growth in 2524 aluminum alloy." *International Journal of Fatigue*, Vol. 24, (2016), 9-16, <https://doi.org/10.1016/j.ijfatigue.2015.11.011>.
23. Yang, B., Wu, M., Li, X., Zhang, J., Wang, H. "Effects of cold working and corrosion on fatigue properties and fracture behaviors of precipitate strengthened Cu-Ni-Si alloy." *International Journal of Fatigue*, Vol. 116, (2018), 118-127, <https://doi.org/10.1016/j.ijfatigue.2018.06.017>.
24. Gavras, A.G., Lados, D.A., Champagne, V.K., Warren, R.J. "Effects of processing on microstructure and fatigue crack growth mechanisms in cold-spray 6061 aluminum alloy." *International Journal of Fatigue*, Vol. 110, (2018), 49-62, <https://doi.org/10.1016/j.ijfatigue.2018.01.006>.
25. Shiozaki, T., Tamai, Y., Urabe, T. "Effect of residual stresses on fatigue strength of high strength steel sheets with punched holes." *International Journal of Fatigue*, Vol. 80, (2015), 324-331, <https://doi.org/10.1016/j.ijfatigue.2015.06.018>.
26. Ritchie, R.O., Suresh, S. "Some considerations on fatigue crack closure at near-threshold stress intensities due to fracture surface morphology." *Metallurgical Transaction A*, Vol. 13, (1982), 937-940, <https://doi.org.ezproxy.ugm.ac.id/10.1007/BF02642409>.
27. Suresh, S. "Fatigue crack deflection and fracture surface contact: micromechanical models." *Metallurgy Transaction A*, Vol. 16, (1985), 249-260, <https://doi.org.ezproxy.ugm.ac.id/10.1007/BF02815306>.
28. Ilman, M.N., Sriwijaya, R.A., Muslih, M.R., Triwibowo, N.A., Sehon. "Strength and fatigue crack growth behaviours of metal inert gas AA5083-H116 welded joints under in-process vibrational treatment." *Journal of Manufacturing Processes*, Vol. 59, (2020), 727-738, <https://doi.org/10.1016/j.jmapro.2020.10.035>.
29. Newman Jr, J.C. "The merging of fatigue and fracture mechanics concepts: a historical perspective." *Progress in Aerospace Sciences*, Vol. 34, (1998), 347-390, [https://doi.org/10.1016/S0376-0421\(98\)00006-2](https://doi.org/10.1016/S0376-0421(98)00006-2).
30. Matos, P.P., Moreira, P.P., Pina, J.C. "Residual stress effect on fatigue striation spacing in a cold-worked rivet hole." *Theoretical and Applied Fracture Mechanics*, Vol. 42, (2004), 139-148, <https://doi.org/10.1016/j.tafmec.2004.08.003>.
31. Yan-li, W., You-li, Z., Shui, H., Han-xiao, S., Yong, Z. "Investigation on fatigue performance of cold expansion holes of 6061-&6 aluminum alloy." *International Journal of Fatigue*, Vol. 95, (2017), 216-228, <https://doi.org/10.1016/j.ijfatigue.2016.10.030>.
32. Muñoz-Cubillos, J., Coronado, J.J., Rodríguez, S.A. "Deep rolling effect on fatigue behavior of austenitic stainless steels." *International Journal of Fatigue*, Vol. 95, (2017), 120-131, <https://doi.org/10.1016/j.ijfatigue.2016.10.008>.



## Persian Abstract

## چکیده

در مطالعه حاضر، تأثیر نورد سرد و زمان بازپخت بر رفتار انتشار ترک خستگی آلیاژ آلومینیوم AA5052 بررسی شد. ورق آلیاژ تحت کاهش نوردهای مختلف، به طور مثال 0، 15، 30 و 45 درصد نورد سرد شد. سپس 45٪ نمونه نورد شده در دمای 370 درجه سانتیگراد تحت زمانهای مختلف پخت، به مدت 2، 4 و 6 ساعت آنبیل شد. تکاملهای ریزساختار پس از تیمارهای نورد سرد و بازپخت نیز با استفاده از میکروسکوپ نوری مورد بررسی قرار گرفت در حالی که رفتار انتشار ترک خستگی با استفاده از تست خستگی مشخص شد. نتایج نشان داد که دانه های کاملاً کشیده با افزایش کاهش نورد مشاهده شدند. ریزساختارهای کشیده به دلیل تبلور مجدد در حین عملیات بازپخت به ساختارهای هم محور تغییر یافت. عمر خستگی با افزایش کاهش نورد به شدت کاهش یافت اما با افزایش زمان پخت به طور قابل توجهی افزایش یافت. عمر خستگی آلیاژ با نورد سرد تا 45٪/93٪ کاهش می یابد. از طرف دیگر، عمر خستگی 45٪ نمونه های نورد شده در زمان حرارت دادن در دمای 370 درجه سانتیگراد به مدت 6 ساعت به میزان قابل توجهی 412 درصد افزایش یافت.